

Development of Reactive Methacrylates Based on Glycidyl Methacrylate

OZLEM KARAHAN, KINYAS AYDIN, SEDA EDIZER, NIHAN ODABASI, DUYGU AVCI

Department of Chemistry, Bogazici University, 34342 Bebek, Istanbul, Turkey

Received 5 March 2010; accepted 28 May 2010

DOI: 10.1002/pola.24163

Published online in Wiley InterScience (www.interscience.wiley.com).

ABSTRACT: Six methacrylate monomers have been synthesized for use as reactive diluents in dental composites and evaluated to investigate the relationship between molecular structure and monomer reactivity. Four were synthesized by reactions of glycidyl methacrylate (GMA) with various acids, 2-(2-methoxyethoxy)acetic acid (**1**), 2-(2-(2-methoxyethoxy)ethoxy)acetic acid (**2**), cyanoacetic acid (**3**), and benzoic acid (**4**); others were synthesized by reactions of GMA with diethyl hydrogen phosphate (**5**) or methanol (**6**). Monomers **1** and **2** are novel, **3** seems to be novel, **4** and **6** were synthesized via a novel method, and the synthesis of **5** was described in the literature. The monomers showed high crosslinking tendencies during thermal bulk polymerizations. The photo-, homo-, and copolymerization behavior of the monomers with 2,2-bis[4-(2-hydroxy-3-methacryloyloxy)phenyl]propane (Bis-GMA) were investigated. The

maximum rate of polymerizations of monomers **2–6** was found to be greater than triethyleneglycol dimethacrylate, Bis-GMA, 2-hydroxyethyl methacrylate, and glycerol dimethacrylate. For the more reactive monomers (**2**, **3**, and **4**), the oxygen sensitivity of polymerization was found to be low due to a hydrogen abstraction/chain transfer reaction. The computationally calculated dipole moment and lowest unoccupied molecular orbital energies indicated that there seems to be a correlation between these quantities and reactivity for ester linked monomers (**1–5**), which was also supported by ^{13}C NMR data. © 2010 Wiley Periodicals, Inc. *J Polym Sci Part A: Polym Chem* 48: 3787–3796, 2010

KEYWORDS: crosslinking; dental polymers; glycidyl methacrylate; photopolymerization; radical polymerization

INTRODUCTION Photopolymerization processes have found a large variety of industrial applications, mainly in dental materials, biomaterials, coatings, and photolithography.^{1–3} Acrylate and methacrylate monomers are used in these processes because of their high polymerization rates and excellent final polymer properties.

2,2-Bis[4-(2-hydroxy-3-methacryloyloxy)phenyl]propane (Bis-GMA) is the most common methacrylate used in dental composites due to its high mechanical strength, low volatility, and low polymerization shrinkage. However, it has very high viscosity and low polymerization conversion. Although reactive diluent monomers such as triethyleneglycol dimethacrylate (TEGDMA) are added to decrease viscosity and increase conversion, some drawbacks arise such as increased polymerization shrinkage, cytotoxicity, and water absorption. Therefore, development of highly reactive novel monomers as reactive diluents alternative to TEGDMA with lower water absorption, polymerization shrinkage, and cytotoxicity is one of the most important challenges in this area.

In recent years, several factors leading to the enhanced reactivity of (meth)acrylates were hypothesized. These are hydrogen abstraction from labile hydrogens in monomers, hydrogen bonding, and electronic effects (dipole moment and secondary functionalities).

Decker and Bowman formulated new monoacrylate monomers with carbonate, cyclic carbonate, carbamate, and oxazolidone groups that react extremely rapidly despite one vinyl group and form crosslinked polymers. They mentioned that crosslinking due to hydrogen abstraction reactions causes an increase in viscosity, earlier gelation, and autoacceleration, which lead to high rate of polymerization.^{4–10}

Jansen et al.¹¹ investigated the rate of polymerization of different acrylates in terms of hydrogen bonding capability for systems containing amide, urethane, and urea groups and found that the monomers capable of forming hydrogen bonds show three to six times higher polymerization rates compared with their nonhydrogen bonding analogues possessing ester and carbonate groups. The high reactivities were suggested to be due to preorganization via hydrogen bonding to bring the double bonds close to each other, enhancing the rate of polymerization, although reduction in termination rate may also be involved or be the cause. They also investigated the effect of monomer polarity on rate of polymerization and found a direct correlation between the maximum rate of polymerization and the dipole moment of the monomer above 3.5 Debye. However, Kilambi et al.⁷ found no monotonic correlation between monomer reactivity and molecular dipole moments during bulk polymerization of various acrylate monomers. They suggested that a low

Correspondence to: D. Avci (E-mail: avcid@boun.edu.tr)

Journal of Polymer Science: Part A: Polymer Chemistry, Vol. 48, 3787–3796 (2010) © 2010 Wiley Periodicals, Inc.

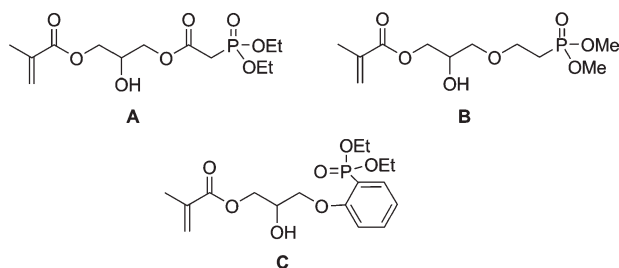


FIGURE 1 Structures of phosphonated methacrylates synthesized from GMA in our previous works.

dipole moment conformation of a monomer may be more reactive due to intermolecular hydrogen bonding than a conformation with a higher dipole moment.

It was observed that the presence of secondary functionalities (carbamates, carbonates, cyclic carbonates, cyclic acetals, morpholine, oxazolidones, hydroxyl, and aromatic rings) enhances reactivity by reducing activation energies in both Michael addition and photopolymerizations indicated by a monotonic correlation between them. The cyclic voltammetry experiments also proved a correlation between reduction potential of the monomers and Michael addition and photopolymerization reactivities.⁵

In our previous works, we synthesized phosphonated methacrylates based on glycidyl methacrylate (GMA) for dental applications (Fig. 1). These monomers showed high polymerization rates and crosslinking tendencies.^{12,13} Unexpectedly, monomers A and C that are monomethacrylates were found to be more reactive than dimethacrylate monomers such as glycerol dimethacrylate (GDMA) and Bis-GMA.

The factors for enhancement of monomer reactivity are not very clear yet, nor is their relative importance. To examine the relationship between monomer structure and reactivity, here, a series of monomers based on GMA and whose structures were changed in the third functionality were designed, synthesized, characterized, and evaluated for their rate of polymerization.

EXPERIMENTAL

Materials

GMA, 2-(2-methoxyethoxy)acetic acid, 2-(2-(2-methoxyethoxy)ethoxy)acetic acid, diethylchlorophosphate, 2,6-di-*tert*-butyl-4-methylphenol (BHT), cyanoacetic acid, benzoic acid, hexyl acrylate (HA), 2-hydroxyethyl methacrylate (HEMA), Bis-GMA, TEGDMA, GDMA, and 2,2-dimethoxy-2-phenylacetophenone (DMPA) were used as received from Aldrich.

Measurements

The monomer characterization involved ¹H and ¹³C NMR spectroscopy (Varian Gemini 400 MHz) and Fourier-transform infrared (FTIR) spectroscopy (T 380). Photopolymerizations were carried out on a TA Instruments Q100 differential photocalorimeter (DPC). Thermogravimetric analysis was done with a TA Instrument (Q50). Viscosity measurements

were carried out using Gemini 150 Rheometer system (Bohlin Instruments).

Synthesis of Monomers

Monomer 1

GMA (1.01 g, 7.1 mmol), 2-(2-methoxyethoxy)acetic acid (0.99 g, 7.40 mmol), BHT (2.6 mg, 0.012 mmol), and triethylamine (TEA) (102.2 mg, 1.0 mmol) were added to a round-bottom flask with a water condenser and nitrogen inlet. The mixture was stirred at 60 °C for 18 h. The purification of the crude product by column chromatography (silica gel 0.063–0.200 mm) using dichloromethane initially and gradually changing to ethyl acetate (EA) as elutant resulted in a light yellow oil in 46.6% yield.

¹H NMR (400 MHz, CDCl₃, δ, ppm): 1.87 (s, 3H, CH₃—C), 3.31 (s, 3H, CH₃—O), 3.51 (t, 2H, CH₂—O), 3.63 (t, 2H, CH₂—O), 4.04–4.30 (m, 7H, CH₂—CH, CH₂—C=O), 5.53, 6.06 (s, 2H, C=CH₂). ¹³C NMR (400 MHz, CDCl₃, δ, ppm): 18.14 (CH₃—C), 58.89 (CH₃—O), 64.97, 65.56 (CH₂—O), 67.64 (CH—OH), 68.38, 70.72 (CH₂—O), 71.82 (CH₂—O—CH₃), 125.89 (CH₂=C), 135.65 (C=CH₂), 167.13 (CH₂=C—C=O), 170.33 (C=O). FTIR (cm⁻¹): 3430 (O—H), 2888 (C—H), 1754 (C=O), 1716 (C=O), 1635 (C=C).

Monomer 2 was obtained with the same procedure using 2-(2-(2-methoxyethoxy)ethoxy)acetic acid. The purification of the crude product by column chromatography (silica gel 0.063–0.200 mm) using hexane initially and gradually changing to ethyl acetate as elutant resulted in a light yellow oil in 49.7% yield. Characterization data are given next.

Monomer 2

¹H NMR (400 MHz, CDCl₃, δ, ppm): 1.92 (s, 3H, CH₃—C), 3.35 (s, 3H, CH₃—O), 3.53–3.80 (m, 8H, CH₂—O), 4.14–4.60 (m, 7H, CH₂—CH, CH₂—C=O), 5.60, 6.13 (s, 2H, CH₂=C). ¹³C NMR (400 MHz, CDCl₃, δ, ppm): 18.18 (CH₃—C), 58.93 (CH₃—O), 64.98, 65.6 (CH₂—O), 67.58 (CH—OH), 68.39, 69.4, 70.72 (CH₂—O), 71.83 (CH₂—O—CH₃), 126.25 (CH₂=C), 135.65 (C=CH₂), 167.15 (CH₂=C—C=O), 170.34 (C=O). FTIR (cm⁻¹): 3432 (O—H), 2883 (C—H), 1753 (C=O), 1716 (C=O), 1635 (C=C).

Monomer 3

GMA (0.99 g, 6.99 mmol), cyanoacetic acid (0.63 g, 7.41 mmol), BHT (2.9 mg, 0.013 mmol), and TEA (99.1 mg, 0.98 mmol) were added to a round-bottom flask with a water condenser and nitrogen inlet and stirred at 40 °C for 5 h. The residue was diluted with CH₂Cl₂ and extracted with NaHCO₃ (5%) solution. After the drying of the organic phase with anhydrous Na₂SO₄ and evaporation of the solvent, the crude product was purified by column chromatography (silica gel 0.063–0.200 mm) using hexane initially and changing to ethyl acetate as elutant. The pure product was obtained as colorless oil in 24.3% yield.

¹H NMR (400 MHz, CDCl₃, δ, ppm): 1.93 (s, 3H, CH₃—C), 3.55 (s, 2H, CH₂—CN), 4.15–4.6 (m, 5H, CH₂—CH, CH), 5.61, 6.12 (s, 2H, CH₂=C). ¹³C NMR (400 MHz, CDCl₃, δ, ppm): 18.14 (CH₃—C), 24.59 (CH₂—CN), 64.89, 67.09 (CH₂—O), 69.42 (CH—OH), 113.06 (CN—CH₂), 126.54 (CH₂=C), 135.54

(C=CH₂), 163.05 (CH₂=C-C=O), 167.27 (C=O). FTIR (cm⁻¹): 3494 (O-H), 2963 (C-H), 1750 (C=O), 1712 (C=O), 1635 (C=C).

Monomer **4** was obtained with the same procedure using benzoic acid. The purification of the crude product by column chromatography (silica gel 0.063–0.200 mm) using hexane initially and gradually changing to ethyl acetate as eluant resulted in a colorless oil in 24.3% yield. Characterization data are given next.

Monomer 4

¹H NMR (400 MHz, CDCl₃, δ, ppm): 1.96 (s, 3H, CH₃), 4.20–4.50 (m, 5H, CH₂-CH), 5.62, 6.16 (s, 2H, CH₂=C), 7.40–7.50 (m, 2H, Ar-CH), 7.50–7.65 (m, 1H, Ar-CH), 8.00–8.15 (m, 2H, Ar-CH). ¹³C NMR (400 MHz, CDCl₃, δ, ppm): 17.97 (CH₃-C), 65.25, 65.47 (CH₂-OH), 67.81 (CH-OH), 126.17 (CH₂=C), 128.17, 129.45, 133.01 (Ar-CH), 135.52 (C=CH₂), 166.41 (CH₂=C-C=O), 167.21 (C=O). FTIR (cm⁻¹): 3432 (O-H), 2958 (C-H), 1714 (C=O), 1636 (C=C).

Monomer 5

Diethylchlorophosphate (5.00 g, 28.9 mmol) and water (3.10 g, 172.2 mmol) were added to a round-bottom flask, and the mixture was stirred at room temperature for 1 h. The solution was extracted with dichloromethane. After the drying of the organic phase and evaporation of the solvent, diethyl hydrogen phosphate was obtained.

The formed product, diethyl hydrogen phosphate (1.75 g, 11.36 mmol) and GMA (1.34 g, 9.43 mmol) were added to a round-bottom flask with a nitrogen inlet. The mixture was stirred at 50 °C for 5 h. The crude product was washed with water, cyclohexane, and petroleum ether and then further purified by column chromatography (silica gel 0.063–0.200 mm) using CH₂Cl₂ initially and gradually changing to 1% methanol in CH₂Cl₂ as eluant. The pure product was obtained as a viscous yellow oil in a 31.5% yield.

¹H NMR (400 MHz, CDCl₃, δ, ppm): 1.34 (s, 3H, CH₃-CH₂), 1.94 (t, 3H, CH₃-C), 2.6 (bs, 1H, OH), 4.07–4.24 (m, 9H, CH₂-CH), 5.59, 6.13 (s, 2H, CH₂=C). ¹³C NMR (400 MHz, CDCl₃, δ, ppm): 16.35 (CH₃-CH₂), 18.59 (CH₃-C), 64.64, 68.92 (CH₂-O), 64.97 (CH₂-CH₃), 69.09 (CH-OH), 126.60 (CH₂=C), 136.06 (C=CH₂), 167.55 (C=O). FTIR (cm⁻¹): 3379 (O-H), 2983 (C-H), 1717 (C=O), 1637 (C=C), 1249 (P=O), 1017 cm⁻¹ (P-O-Et).

Monomer 6

GMA (0.84 g, 5.92 mmol), 30 mL methanol, and Amberlyst-15 (600.4 mg) were added to a round-bottom flask and placed in an ultrasonic bath. After 2 h at 22–30 °C, the catalyst was filtered, methanol was evaporated, and the residue was washed with hexane to remove unreacted GMA. The pure product was obtained as a colorless liquid after column chromatography (silica gel 0.063–0.200 mm), starting CH₂Cl₂ elutant and changing to ethyl acetate: CH₂Cl₂ (20:80) gradually.

¹H NMR (400 MHz, CDCl₃, δ, ppm): 1.95 (s, 3H, CH₃-C), 3.4–3.6 (m, 5H, CH₃-O, CH₂-O-CH₃), 4.00–4.40 (m, 3H,

CH-OH, CH₂-O), 5.59, 6.13 (s, 2H, CH₂=C). ¹³C NMR (400 MHz, CDCl₃, δ, ppm): δ=18.25 (CH₃-C), 59.20 (CH₃-O), 65.69, 68.73 (CH₂-O), 73.43 (CH-OH), 126.01 (CH₂=C), 135.92 (C=CH₂), 167.40 (C=O), 170.34 (C=O). FTIR (cm⁻¹): 3434 (O-H), 2929 (C-H), 1715 (C=O), 1635 (C=C).

Polymerization Procedure

Approximately 3.0 or 4.0 mg of sample was placed in an aluminum differential scanning calorimeter (DSC) pan. The photoinitiator (DMPA), which was dissolved in CH₂Cl₂ was added with a microsyringe to give a final concentration in the monomer of 2.0 mol percent after evaporation of the solvent. The sample and the reference pans were placed in the DSC chamber, the system was purged with nitrogen flow to remove air and CH₂Cl₂ for 10 min before polymerization and purging was continued during polymerization. Heats of photoreactions were measured using a DPC equipped with a mercury arc lamp. The samples were irradiated for 10 min at 40 °C with an incident light intensity of 20 mW cm⁻². The heat flux as a function of reaction time was monitored using DSC under isothermal conditions and both the rate of polymerization (*R_p*) and conversion were calculated as a function of time. The theoretical values used for the heats of reaction (ΔH_p) were 13.1 and 20.6 kcal mol⁻¹ and for methacrylate and acrylate double bonds.^{14,15} Rates of polymerization were calculated according to the following formula:

$$\text{Rate} = \frac{(Qs^{-1})M}{n\Delta H_p m}$$

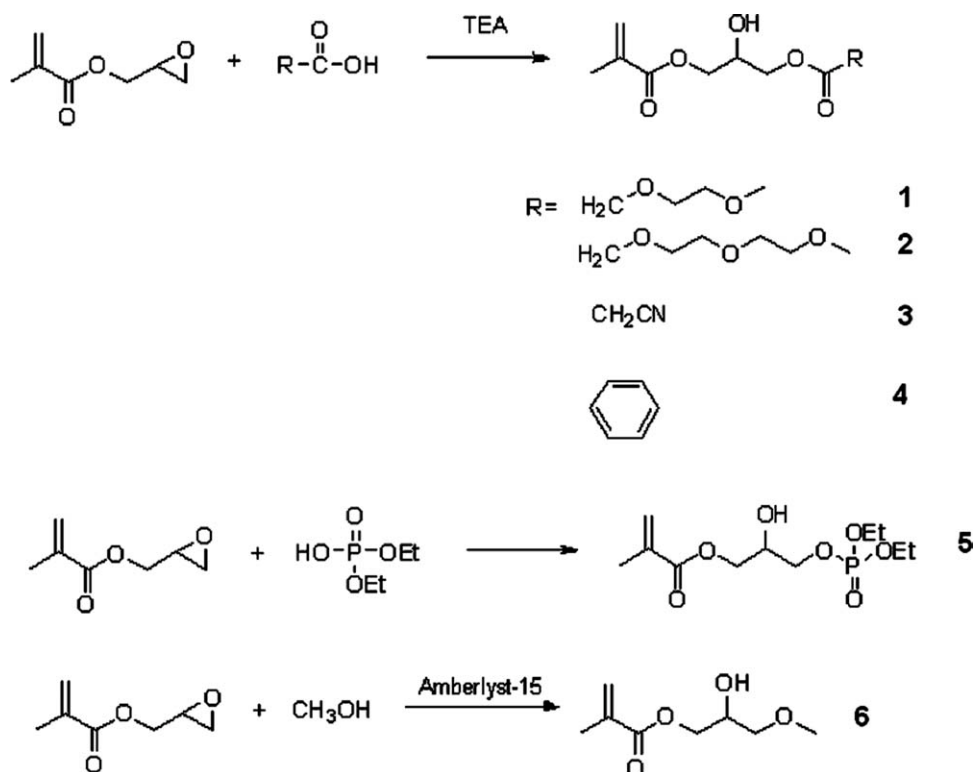
where $Q \text{ s}^{-1}$ is heat flow per second, M the molar mass of the monomer, n the number of double bonds per monomer molecule, ΔH_p is the heat released per mole of double bonds reacted, and m the mass of monomer in the sample.

Computational Simulation

All monomers were fully optimized by density functional theory (DFT) using Gaussian 03 program at the B3LYP/6-31+G(d) to obtain some quantum chemical descriptor to find experimental and computational correlation.¹⁶ Four descriptors were calculated, which are dipole moment, the energy of the lowest unoccupied molecular orbital (E_{LUMO}), natural bond orbital (NBO) charges of the carbon alpha to the carbonyl group, and terminal vinylic carbon.

Calculation of Dipole Moments

Boltzman-averaged dipole moments (μ_{calc}) were calculated using the following method. First, all free rotations around single bonds were considered for a given monomer. Spartan '04 program was used to calculate the Boltzmann-averaged dipole moments.¹⁷ The number of conformations generated is dependent on both the number of bonds and their types. All these conformations were minimized at the PM3 level of theory. The convergence criterion for the maximum gradient was 0.0001 a.u., and the maximum number of geometry optimization cycles was taken to be 20 + the number of independent geometrical parameters for geometry optimization. The unique structures were sorted in the order of increasing energy. The dipole moments of


FIGURE 2 Synthesis of monomers.

the first 100 conformers are Boltzmann averaged at 298.15 K according to the following formula:

$$\langle \mu_{\text{calc}} \rangle = \sum_j D_j \frac{e^{\Delta H_j/RT}}{\sum_i e^{\Delta H_i/RT}} = \sum_j D_j p_j,$$

where D_j is the dipole moment of the conformation j , ΔH_j is the difference between the heat of formation of conformation j and the heat of formation of the global minimum conformation, T is the absolute temperature, R is the ideal gas constant, and p_j is the probability of finding the monomer in conformation j at the temperature T .¹¹

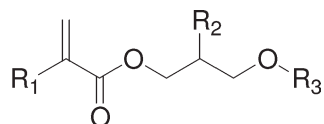
Calculation of E_{LUMO} and NBO Charges

E_{LUMO} and NBO charges of vinylic carbon atoms have been performed with the Gaussian03 package at the B3LYP/6-31+G(d) level.

RESULTS AND DISCUSSION

Monomer Synthesis and Characterization

The ring-opening reaction of GMA with four carboxylic acids, a phosphoric acid derivative, and an alcohol was used for the preparation of new functional monomers with the following structure:



where R_1 is methyl due to methacrylates, R_2 is a secondary functionality that is an OH group, and R_3 is a third

functionality. The hydrogen bonding ability of the monomers will be similar due to OH group. The structure of the third functionality is varied to obtain highly polar monomers.

The general procedure for the synthesis of monomers 1–4 involved a simple one-step ring-opening reaction of GMA with different acids in the presence of TEA as catalyst (Fig. 2). The following acids were used to provide monomers with high polarities: 2-(2-methoxyethoxy)acetic acid, 2-(2-(2-methoxyethoxy)ethoxy)acetic acid, cyanoacetic acid, and benzoic acid. Monomers 1 and 2 are novel, 3 seems to be novel (we could not find its synthesis procedure¹⁸). In the literature, monomer 4 was synthesized using tetrabutylammonium bromide as catalyst in acetonitrile.¹⁹ The reactions were conducted at 60 °C, and BHT was used to prevent homopolymerization of GMA during reactions. Monomers were obtained as viscous oils after purification with column chromatography. The solubilities and viscosities of the monomers are reported in Table 1. All of the synthesized monomers were found to be more viscous than TEGDMA due to hydrogen bonding.

Monomer 5 was synthesized with a procedure similar to that given in the literature.²⁰ GMA was reacted with diethyl hydrogen phosphate, which was prepared from the reaction of diethylchlorophosphate and water (Fig. 2). The pure product was obtained after column chromatography as a colorless oil. It was soluble almost in all organic solvents except hexane, and it was also soluble in water (Table 1).

The ring-opening reaction of the epoxides is not regiospecific. There are two possible sites for attack of alcohols, acids, and anhydrides.^{21,22} If the attack occurs from the less-

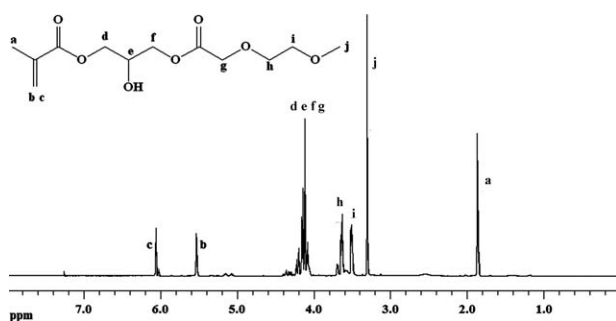
TABLE 1 Viscosities and Solubilities of the Synthesized Monomers and TEGDMA

Monomer	Viscosity (Pa s)	H ₂ O	Ether	Methanol	CH ₂ Cl ₂	THF	Hexane	Acetone
TEGDMA	0.009	–	+	+	+	+	+	+
1	0.047	+	+	+	+	+	–	+
2	0.072	+	+	+	+	+	–	+
3	0.960	–	+	+	+	+	–	+
4	0.258	–	+	+	+	+	–	+
5	0.059	+	+	+	+	+	–	+
6	0.136	±	–	+	+	+	–	+

hindered side, the linear isomer is obtained otherwise the branched isomer or both isomers are produced. The crude product yields of acid reactions were very high, containing mostly the linear isomer with different amounts of the branched isomer.

The ¹H NMR of monomer **1** showed methyl protons at 1.87 ppm, methoxy protons at 3.31 ppm, two methylene protons at 3.51 and 3.63 ppm, other methylene and methine protons between 4.04 and 4.30 ppm, and double bond protons at 5.53 and 6.06 ppm (Fig. 3). The small peaks ~4.4, 5.2, and 6.0 ppm are due to the branched isomer. The ratios of linear to branched isomers for monomers **1**, **2**, and **5** were found to be greater than 7.5:1.

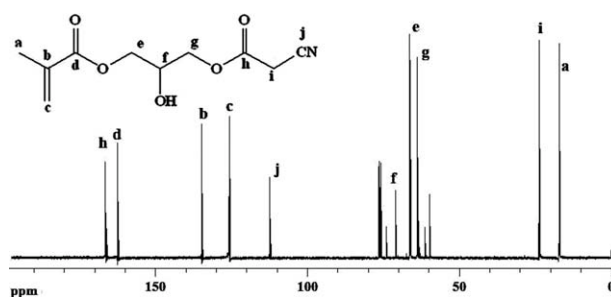
The ¹³C NMR spectrum of monomers **3** and **4** also showed two isomers (Figs. 4 and 5). For example, the spectrum of monomer **4** showed characteristic peaks for methyl carbon at 17.97 ppm, a tertiary carbon at 67.81 ppm, methylene carbons at 65.25 and 65.47 ppm, double bond carbons at 126.20 and 135.52 ppm, aromatic carbons at 128.17, 129.45, and 133.01 ppm, and carbonyl carbons at 166.41 and 167.21 ppm (Fig. 5). The small peaks at 61.02 (CH₂) and 62.75 (CH₂) ppm are due to the branched isomer; small CH peak is difficult to see. The ratio of CH₂ peaks for linear isomer to that of branched isomer indicates relative ratios of the isomers, which is about 4:1. This ratio was also confirmed by ¹H NMR. Another fraction of column chromatography indicated a ratio of 14:1. Similarly, the ratio of linear to branched isomers for monomer **3** was also found to be high (4:1). These results indicated the amount of branched isomers formed is greater for the acids with more rigid structures.

**FIGURE 3** ¹H NMR of monomer **1**.

The FTIR spectra of the monomers **1–4** showed the presence of alcoholic OH bond at ~3400 cm⁻¹, the double bonds at 1634 cm⁻¹, two different ester C=O bonds at ~1750 and 1716 cm⁻¹ (Fig. 6) except monomer **4** where two C=O peaks overlap at 1713 cm⁻¹. Monomer **5** showed one C=O peak at 1717 cm⁻¹ and also showed P=O and P–OEt group peaks at 1249 and 1017 cm⁻¹.

The alcoholysis of epoxides is conducted under acidic and basic conditions and requires long reaction times and high temperature. Liu et al.²³ have demonstrated that Amberlyst-15 is an efficient heterogeneous catalyst for the regioselective ring-opening reactions of epoxides (such as phenyl glycidyl ether, styrene oxide, and cyclohexene oxide) by alcohols in the formation of β-alkoxy alcohols under ultrasonication at room temperature. We used the same method for the synthesis of our last monomer (monomer **6**; Fig. 2). GMA was reacted with methanol in the presence of Amberlyst-15 in an ultrasonic bath at 25–30 °C. However, the major product was found to be a α-alkoxy alcohol (linear isomer: 78%) with a small amount of β-alkoxy alcohol (branched isomer: 22%) determined from ¹H NMR of the crude product. In the literature, the reaction of GMA with methanol at room temperature using BF₃ as catalyst gave a mixture of products with similar regioselectivity (branched:linear 20/80%).^{24,25}

When the crude product was subjected to a chromatographic separation on silica gel, fractions containing mixture of isomers were obtained. The ¹³H NMR spectra of three isomer mixtures were shown at Figure 7. The ratio of double bond peaks or double bond to CH peak of branched isomer (~5.0 ppm) indicates relative ratios of the isomers. Mixture 1 contains mainly the linear isomer with a very small amount of branched isomer. Mixtures 2 and mixture 3 contain linear to

**FIGURE 4** ¹³C NMR of monomer **3**.

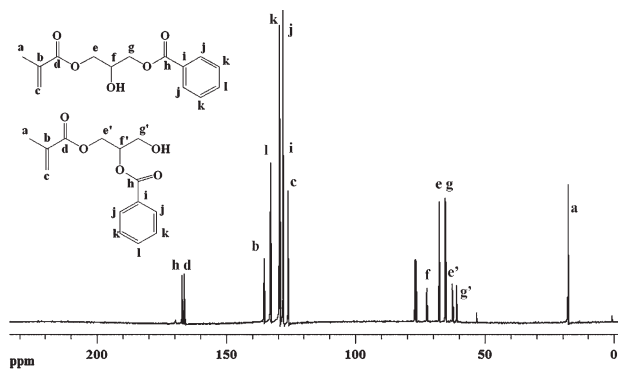


FIGURE 5 ^{13}C NMR of monomer 4.

branched isomers with the ratio of 3.4:1 and 1:1. The FTIR spectrum of this monomer showed the characteristic peaks of hydroxyl, carbonyl, and C=C groups at 3434, 1715, and 1635 cm^{-1} .

Thermal Polymerizations

Bulk polymerizations of monomers 1–6 were carried out with azobisisobutyronitrile (AIBN) (0.5 wt %) at 60 °C. These monomers polymerized very fast to give crosslinked polymers, as indicated by swelling in various solvents. This behavior can be explained by a hydrogen abstraction chain transfer mechanism from the labile hydrogens on the carbons attached to oxygen, which can be followed by reinitiation. The crosslinking will result high mechanical properties, which is an important property for dental materials.

The crosslinked polymer obtained from monomer 5 may also have potential as flame retardant due to its phosphate

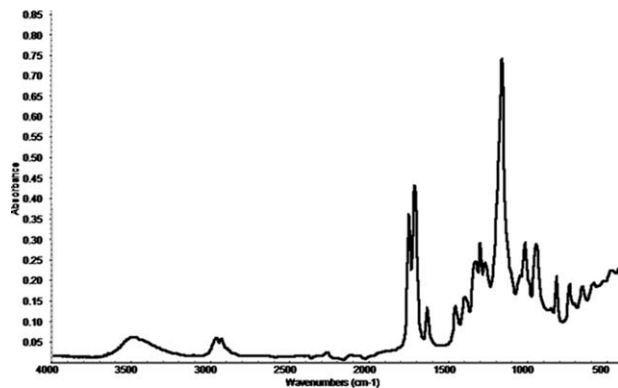


FIGURE 6 FTIR spectrum of monomer 3.

group. The thermal gravimetric analysis of this polymer (residual monomer was removed by several washings with methylene chloride) showed a major weight loss ~ 270 °C and a char yield of 33.3%. This char yield was higher than those of GMA-based crosslinked phosphonated polymers (poly-A, poly-B, and poly-C) with the char yields of 25–30%. The enhanced char production of phosphates compared with phosphonates is due to formed phosphoric acid, which is more effective at promoting further crosslinking of polymers instead of the weaker phosphonic acid.²⁶

Photopolymerization

Photopolymerization of the monomers were followed by DPC. First, the homopolymerization behavior of the synthesized monomers was investigated and compared with those of commercial monomers such as HEMA, Bis-GMA, GDMA,

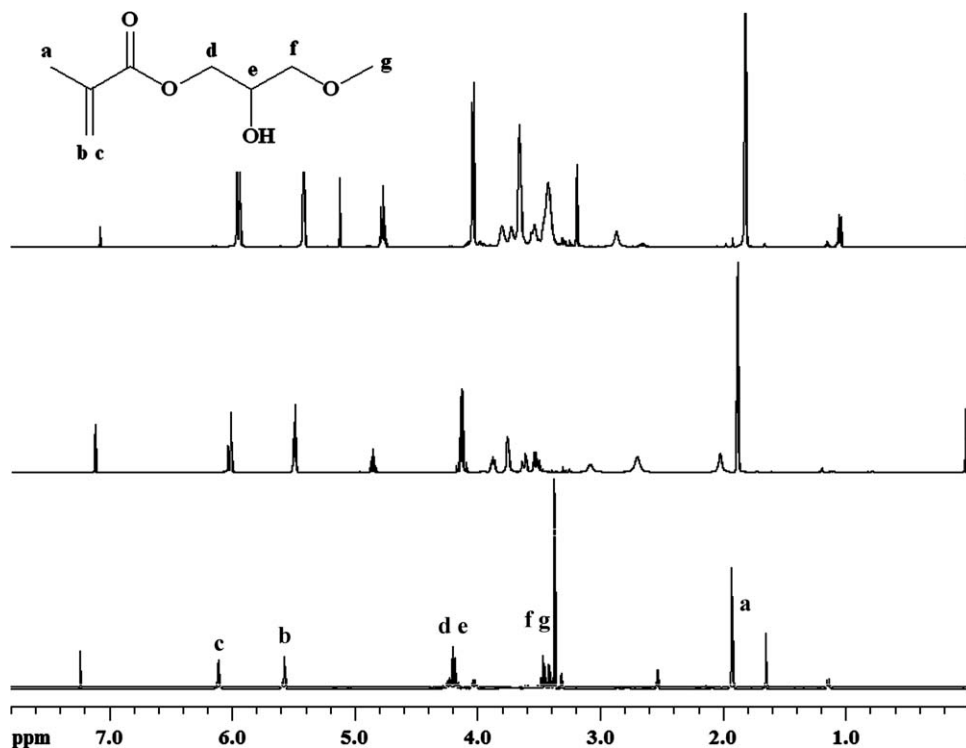


FIGURE 7 ^1H NMR of isomer mixtures of monomer 6 (mixture 1-bottom, mixture 2-middle, and mixture 3-top).

TABLE 2 Rate of Polymerizations and Conversions of Monomers 1–6, Bis-GMA, TEGDMA, HEMA, and GDMA

Monomer (Linear:Branched)	R_p (s^{-1})	Conversion (%)
1 (>7.5:1)	0.034 ± 0.003	91 ± 3
2 (>7.5:1)	0.060 ± 0.001	95 ± 2
3 (5:1)	0.074 ± 0.002	88 ± 2
4 (14:1)	0.070 ± 0.002	72 ± 2
4 (4:1)	0.061 ± 0.002	74 ± 2
5 (>7.5:1)	0.066 ± 0.003	64 ± 3
6 (>7.5:1)	0.065 ± 0.001	81 ± 3
6 (1:1)	0.058 ± 0.001	68 ± 1
TEGDMA	0.056 ± 0.002	79 ± 2
Bis-GMA	0.037 ± 0.003	47 ± 2
HEMA	0.037 ± 0.002	92 ± 1
GDMA	0.040 ± 0.00	58 ± 1

and TEGDMA. Table 2 shows the results in terms of rate of polymerizations and conversions.

It is known that, as the monomer functionality increases, the rate of polymerization increases while the conversion decreases. However, the synthesized monofunctional monomers except one (monomer **1**) showed higher rates of polymerization (0.058 – $0.074 s^{-1}$) than Bis-GMA ($0.037 s^{-1}$) and GDMA ($0.040 s^{-1}$) and similar or higher rates of polymerization than TEGDMA ($0.056 s^{-1}$). In addition to hydrogen abstraction mechanism, the high reactivity of the synthesized monomers can be explained by their hydrogen bonding capabilities leading to high viscosity and earlier Trommsdorff effect. Monomer **1** was found to be the least reactive monomer, which also correlates with its low viscosity, as expected. These properties may be understood to be due to a combination of low dipole moment (in dipole moment section) and low hydrogen bonding capability. The conversions of all the synthesized monomers (64–95%) were higher than Bis-GMA (47%) and GDMA (58%). Monomers **1** and **2** with very flexible structure gave very high conversions (91 and 95%).

It was observed that the rate and conversion data of a given monomer is different for different fractions of column chromatography, which indicated different reactivities of the two isomers. To see the effect of isomer structure on the rate of polymerization, two fractions obtained from column chromatography of monomer **4** and **6** were polymerized. It was observed that as the branched isomer content in the isomer mixture is increased, the maximum rate of polymerization is decreased. For example, the maximum rate of polymerization of monomer **4** decreased from 0.070 (14:1, linear:branched) to $0.061 s^{-1}$ (4:1, linear:branched). Similarly, rates were found to be 0.065 (mixture 1) and $0.058 s^{-1}$ (mixture 3) for two different isomer mixtures of monomer **6**. We observed similar behavior during polymerizations of ethyl α -chloromethacrylate-GDMA isomer mixtures.²⁷ The reason for the higher reactivity of the linear isomers is not obvious. We suggest an explanation by the polarity differences of isomers in the next section.

The synthesized monomers were also evaluated as reactive diluents to Bis-GMA. The maximum rate and conversion values of Bis-GMA:monomer (50:50 mol %) mixtures were measured and compared with a control Bis-GMA:TEGDMA (50:50 mol %) system. It was observed that on addition of monomers (except monomer **1**), both maximum rate of polymerizations and conversions were improved, and the values are comparable with the control (Table 3). We could not explain why addition of a very flexible monomer (monomer **1**) to Bis-GMA did not increase the conversion. The maximum rate of polymerization and conversion of the mixtures (except Bis-GMA:**1**) were between the rates of polymerizations and conversions of the two monomers. For example, the maximum rate of polymerization of Bis-GMA and monomer **2** were 0.037 and $0.060 s^{-1}$, whereas the mixtures of Bis-GMA with monomer **2** gave maximum rate of polymerization of $0.056 s^{-1}$.

Effect of Monomer Structure on Oxygen Inhibition

Although free radical polymerizations are inhibited by oxygen, most of the curing processes are conducted in air. The presence of oxygen results in long induction times, low conversions, slow polymerization rates, short chains, and poor polymer properties.²⁸ In general, oxygen inhibition depends on viscosity of the medium that is effected by monomer functionality, molecular weight, and functional groups present in the monomer structure (such as OH). When the viscosity is high or increases during polymerization, diffusion rate of oxygen to the monomer will be low. Other than viscosity, monomers with abstractable hydrogens such as ether groups were showed to reduce oxygen inhibition by forming peroxy radical. For example, Hoyle and coworkers found that TEGDMA shows oxygen inhibition in air with less than 15% decrease in polymerization rate, while 1,12-dodecane dimethacrylate shows $\sim 35\%$ reduction in rate. They also concluded that methacrylates were less sensitive to oxygen than acrylates. The reduction of rate of polymerization of HA was found to be $\sim 80\%$.²⁸

Since we propose a hydrogen abstraction mechanism for the formation of crosslinked structures from our monomers, we investigated their photopolymerization behavior in the presence and absence of oxygen. Figures 8 and 9 show the polymerization exotherms and conversions of monomer **2** together with HA in the presence and absence of oxygen. The

TABLE 3 Rate of Copolymerizations and Conversions of Monomers 1-6 and TEGDMA with Bis-GMA

Monomers (50:50 mol %)	R_p (s^{-1})	Conversion (%)
Bis-GMA: 1	0.035 ± 0.002	43 ± 2
Bis-GMA: 2	0.056 ± 0.003	70 ± 2
Bis-GMA: 3	0.040 ± 0.03	50 ± 2
Bis-GMA: 4	0.050 ± 0.003	57 ± 2
Bis-GMA: 5	0.043 ± 0.001	57 ± 2
Bis-GMA: 6	0.049 ± 0.002	52 ± 3
Bis-GMA:TEGDMA	0.052 ± 0.003	56 ± 3

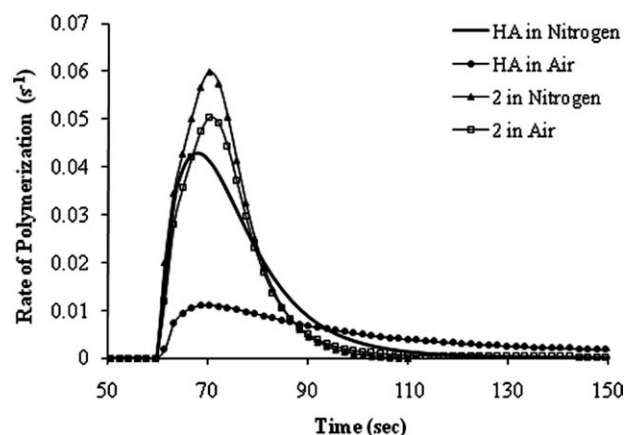


FIGURE 8 Photopolymerization rate versus time for monomer **2** and HA in nitrogen and air.

photopolymerization results of monomers **2**, **3**, and **4** were listed in Table 4. The synthesized monomers showed little oxygen inhibition in air (10–13% decrease in rate), whereas HA (76% decrease in air) was found to be very sensitive to air. These findings support our proposed hydrogen abstraction chain transfer mechanism.

Dipole Moment

The synthesized monomers were evaluated in terms of dipole moment to find a relation between monomer structure and reactivity. The Boltzmann-averaged dipole moments of monomers were calculated for minimum energy conformers (Table 5). When we consider ester linked monomers (**1**–**5**), there seems to be a correlation: the most reactive monomer has the highest dipole moment, the least reactive one, lowest; with the other three in between (the intermediate ones are too close together for their differences to have meaning).

We also calculated dipole moments of some of the branched isomers. They were found to be lower than those of the linear isomers as expected. For example, linear isomers of monomers **3**, **4**, and **6** were found to have dipole moments of 5.30, 3.97, and 3.04, whereas branched isomers gave val-

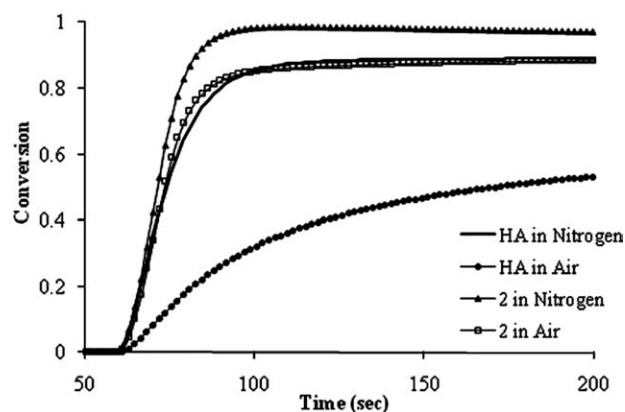


FIGURE 9 Conversion versus time for monomer **2** and HA in nitrogen and air.

TABLE 4 Photopolymerization Rates and Conversions of Monomers **2**, **3**, **4**, and HA in the Presence and Absence of Oxygen

Monomer	R_p (s^{-1})	Conversion (%)
2	0.060 ± 0.001	95 ± 2
2 ^a	0.050 ± 0.002	89 ± 2
3	0.074 ± 0.002	88 ± 2
3 ^a	0.069 ± 0.002	80 ± 2
4	0.070 ± 0.002	72 ± 2
4 ^a	0.061 ± 0.001	75 ± 2
HA	0.043 ± 0.003	82 ± 4
HA ^a	0.010 ± 0.002	60 ± 2

^a In air.

ues of 3.49, 3.22, and 2.82 (Table 5). The difference for monomer **3** was very significant, which may explain the lower reactivity of monomer **3** (isomer mixture) than expected.

Calculation of NBO Charges and E_{LUMO}

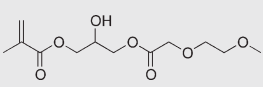
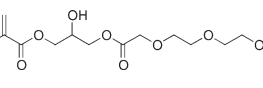
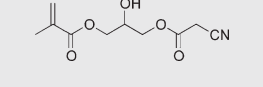
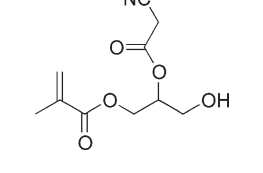
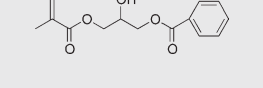
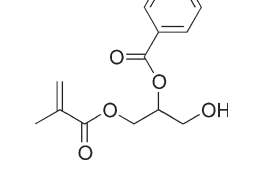
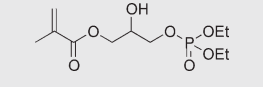
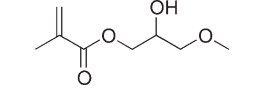
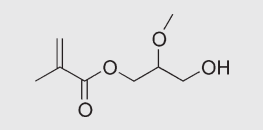
Computer simulations were used to observe the electron density surfaces and partial charges on double bond carbons of the synthesized monomers. These values were compared with the chemical shift differences of these carbons determined by ^{13}C NMR spectra.

The calculated charges on the terminal vinyl carbons and the carbon alpha to the carbonyl group of the monomers were similar to indicate a correlation with reactivities (Table 5).

Bowman and coworkers⁵ said that a molecule with smaller E_{LUMO} value shows higher susceptibility toward attack by nucleophiles or radicals. Thus, during a polymerization of a monomer with a lower LUMO energy, the activation energy for the propagation is reduced, which results in an increase in rate of polymerization. We also calculated the LUMO energies of the synthesized monomers using B3LYP DFT to explain reactivity differences between them (Table 5). We observed a correlation between the polymerization rate and LUMO energies for the ester linked monomers (**1**–**5**); the most reactive monomer (monomer **3**) has the lowest LUMO energy, whereas the least reactive one (monomer **1**) has the highest LUMO energy. The ether linked monomer with the highest LUMO energy did not follow this trend.

^{13}C NMR can be used to predict free radical polymerizability of monomers. The chemical shift differences of the C=C double bonds ($C_\beta H_2=C_\alpha^-$) of the synthesized monomers are given in Table 5. Vaidya et al. have reported that δC_β and δC_α shift to lower and higher fields, respectively, with an increase in electron withdrawing power of the substituents. Therefore, $\Delta\delta$ ($\delta C_\beta - \delta C_\alpha$) shows the effects of substituents on polymerizability. The stronger the electron-withdrawing power of the substituents, the smaller the difference and the higher the radical polymerizability.^{29,30} Also, bulky substituents may cause differences in chemical shifts and/or lead to lower propagation enthalpy through steric hindrance. Comparison

TABLE 5 Dipole Moments, Chemical Shift Differences, LUMO Energies, and NBO Charges of the Monomers

Monomer	Dipole Moment	$\Delta\delta$	LUMO Energies (eV)	Charges on the Terminal Vinylic Carbon	Charges on the Carbon Alpha to the Carbonyl Group
	2.81	9.76	-0.06817	-0.3749	-0.1238
	3.94	9.40	-0.07487	-0.3659	-0.1302
	5.30	9.00	-0.08463	-0.3733	-0.1301
	3.49	-	-0.07391	-0.3894	-0.1247
	3.97	9.35	-0.07198	-0.3877	-0.1235
	3.22	-	-0.06757	-0.3713	-0.1206
	3.34	9.50	-0.07361	-0.3872	-0.1243
	3.04	9.91	-0.06295	-0.3879	-0.1268
	2.82	-	-0.06295	-0.3719	-0.1243

of the $\Delta\delta$ values of the ester-linked monomers shows that the most reactive monomer (monomer **3**) has the lowest (9.0 ppm) value and the least reactive one (monomer **1**) has the highest value (9.76 ppm). The monomers with similar polymerization tendencies gave values in between (9.35–9.50). The aforementioned correlation was not applicable to the ether-linked monomer **6**.

CONCLUSIONS

Six hydroxyl-containing methacrylate monomers with various third functionalities were synthesized as mixtures of isomers. Photopolymerization studies of these monomers indicated that the monomers they can be used as alternative reactive diluent to TEGDMA in Bis-GMA. Monomer **2** was found to be the best monomer between all the monomers studied. Low sensitivity of the monomers to oxygen is consistent with the crosslinked polymer formation during thermal polymerization due to a proposed hydrogen abstraction chain transfer reaction. Although we could not see a monotonic correlation between computationally calculated dipole moment and LUMO energies, these values can be used to roughly estimate relative reactivities of the monomers with similar structures.

The authors thank Viktorya Aviyente for valuable suggestions during computational work and Oguz Okay and Deniz Ceylan for viscosity measurements.

REFERENCES AND NOTES

- Kloosterboer, J. G. *Adv Polym Sci* 1988, 84, 1–61.
- Decker, C.; Elzaouk, B. *J Appl Polym Sci* 1997, 65, 833–844.
- Anseth, K. S.; Newman, S. M.; Bowman, C. N. *Adv Polym Sci* 1995, 122, 177–217.
- Moussa, K.; Decker, C. *J Polym Sci Polym Part A: Polym Chem* 1993, 31, 2197–2203.
- Kilambi, H.; Reddy, S. K.; Schneidewind, L.; Stansbury, J. W.; Bowman, N. C. *J Polym Sci Polym Part A: Polym Chem* 2009, 47, 4859–4870.
- Lu, H.; Stansbury, J. W.; Nie, J.; Berchtold, K. A.; Bowman, N. C. *Biomaterials* 2005, 26, 1329–1336.
- Kilambi, H.; Beckel, E. R.; Berchtold, K. A.; Stansbury, J. W.; Bowman, N. C. *Polymer* 2005, 46, 4735–4742.
- Berchtold, K. A.; Nie, J.; Stansbury, J. W.; Hacioglu, B.; Beckel, E. R.; Bowman, N. C. *Macromolecules* 2004, 37, 3165–3179.
- Beckel, E. R.; Stansbury, J. W.; Bowman, N. C. *Macromolecules* 2005, 38, 9474–9481.
- Beckel, E. R.; Nie, J.; Stansbury, J. W.; Bowman, N. C. *Macromolecules* 2004, 37, 4062–4069.
- Jansen, J. F. G. A.; Dias, A. A.; Dorschu, M.; Coussens, B. *Macromolecules* 2003, 36, 3861–3873.
- Yeniad, B.; Albayrak, A. Z.; Olcum, N. C.; Avci, D. *J Polym Sci Part A: Polym Chem* 2008, 46, 2290–2299.
- Sahin, G.; Avci, D.; Karahan, O.; Moszner, N. *J Appl Polym Sci* 2009, 114, 97–106.
- Anseth, K. S.; Wang, C. M.; Bowman, C. N. *Macromolecules* 1994, 27, 650–655.
- Brandrup, J.; Immergut, E. H. *Polymer Handbook*; Wiley Interscience: New York, 1975.
- Frisch, M. J.; Trucks, G. W.; Schlegel, H. B.; Scuseria, G. E.; Robb, M. A.; Cheeseman, J. R.; Montgomery, J. A., Jr.; Vreven, T.; Kudin, K. N.; Burant, J. C.; Millam, J. M.; Iyengar, S. S.; Tomasi, J.; Barone, V.; Mennucci, B.; Cossi, M.; Scalmani, G.; Rega, N.; Petersson, G. A.; Nakatsuji, H.; Hada, M.; Ehara, M.; Toyota, K.; Fukuda, R.; Hasegawa, J.; Ishida, M.; Nakajima, T.; Honda, Y.; Kitao, O.; Nakai, H.; Klene, M.; Li, X.; Knox, J. E.; Hratchian, H. P.; Cross, J. B.; Bakken, V.; Adamo, C.; Jaramillo, J.; Gomperts, R.; Stratmann, R. E.; Yazyev, O.; Austin, A. J.; Cammi, R.; Pomelli, C.; Ochterski, J. W.; Ayala, P. Y.; Morokuma, K.; Voth, G. A.; Salvador, P.; Dannenberg, J. J.; Zakrzewski, V. G.; Dapprich, S.; Daniels, A. D.; Strain, M. C.; Farkas, O.; Malick, D. K.; Rabuck, A. D.; Raghavachari, K.; Foresman, J. B.; Ortiz, J. V.; Cui, Q.; Baboul, A. G.; Clifford, S.; Cioslowski, J.; Stefanov, B. B.; Liu, G.; Liashenko, A.; Piskorz, P.; Komaromi, I.; Martin, R. L.; Fox, D. J.; Keith, T.; Al-Laham, M. A.; Peng, C. Y.; Nanayakkara, A.; Challacombe, M.; Gill, P. M. W.; Johnson, B.; Chen, W.; Wong, M. W.; Gonzalez, C.; Pople, J. A. *Gaussian 03, Revision D. 01*; Gaussian, Inc.: Wallingford, CT, 2004.
- SPARTAN Version 4.0; Wavefunction, Inc.: Irvine, CA, 1995.
- Naoki, Y.; Junji, Y.; Motoyoshi, Y. *Jpn. Kokai Tokkyo Koho, JP 58098313*, 1983.
- Khalafi-Nezhad, A.; Soltani Rad, M. N.; Khoshnood, A. *Synthesis* 2003, 16, 2552–2558.
- Van Den Bergen, H.; Vanovervelt, J.-C. WO 01/74826 A1, 2001.
- Tamaresevely, K.; Rueggeberg, F. A. *J Appl Polym Sci* 1995, 57, 705–716.
- Davy, K. W. M.; Kalachandra, S.; Pandain, M. S.; Braden, M. *Biomaterials* 1998, 19, 2007–2014.
- Liu, Y.-H.; Liu, Q.-S.; Zhang, Z.-H. *J Mol Catal A* 2008, 296, 42–46.
- Olszewski-Ortar, A.; Gros, P.; Fort, Y. *Tetrahedron Lett* 1997, 38, 8699–8702.
- Caubere, P.; Fort, Y.; Ortar, A. (Atochem Invs). U.S. Patent 5,283,360, 1994.
- Price, D.; Cunliffe, L. K.; Bullet, K. J.; Hull, T. R.; Milnes, G. J.; Ebdon, J. R.; Hunt, B. J.; Joseph, P. *Polym Adv Technol* 2008, 19, 710–723.
- Avci, D.; Mathias, L. J. *Polymer* 2004, 45, 1763–1769.
- Lee, T. Y.; Guymon, C. A.; Jonsson, E. S.; Hoyle, C. E. *Polymer* 2004, 45, 6155–6162.
- Vaidya, R. A.; Mathias, L. J. *J Polym Sci Polym Symp* 1986, 74, 243–251.
- Kodaira, T.; Fujisawa, T.; Liu, Q.-Q.; Urushisaki, M. *Macromolecules* 1996, 29, 484–485.